ACS APPLIED MATERIALS & INTERFACES

Research Article

www.acsami.org

Study of Bacterial Adhesion on Biomimetic Temperature Responsive Glycopolymer Surfaces

Yinan Wang,[†,‡] Yohei Kotsuchibashi,[†,§] Yang Liu,*[,‡] and Ravin Narain*[,†]

[†]Department of Chemical and Materials Engineering, University of Alberta, 116 St and 85 Ave, Edmonton, Alberta T6G 2G6, Canada

[‡]Department of Civil and Environmental Engineering, University of Alberta, 116 St and 85 Ave, Edmonton, Alberta T6G 2G6, Canada

[§]International Center for Materials Nanoarchitectonics (MANA), National Institute for Materials Science (NIMS), 1-1 Namiki, Tsukuba, Ibaraki 305-0044, Japan

Supporting Information

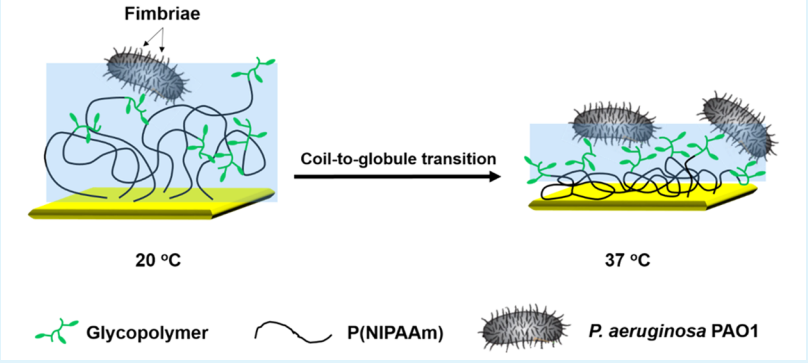

ABSTRACT: *Pseudomonas aeruginosa* is an opportunistic pathogen responsible for diseases such as bacteremia, chronic lung infection, and acute ulcerative keratitis. *P. aeruginosa* induced diseases can be fatal as the exotoxins and endotoxins released by the bacterium continue to damage host tissues even after the administration of antibiotics. As bacterial adhesion on cell surfaces is the first step in bacterial based pathogen infections, the control of bacteria−cell interactions is a worthwhile research target. In this work, thermally responsive poly(*N*-isopropylacrylamide) [P(NIPAAm)] based biomimetic surfaces were developed to study the two major bacterial infection mechanisms, which is believed to be mediated by hydrophobic or lectin−carbohydrate interactions, using quartz crystal microbalance with dissipation. Although, a greater number of *P. aeruginosa* adhered to the NIPAAm homopolymer modified surfaces at temperatures higher than the lower critical solution temperature (LCST), the bacterium−substratum bond stiffness was stronger between *P. aeruginosa* and a galactose based P(NIPAAm) surface. The high bacterial adhesion bond stiffness observed on the galactose based thermally responsive surface at 37 °C might suggest that both hydrophobic and lectin−carbohydrate interactions contribute to bacterial adhesion on cell surfaces. Our investigation also suggests that the lectin−carbohydrate interaction play a significant role in bacterial infections.

KEYWORDS: *QCM-D, glycopolymers, P(NIPAAm), lectin−carbohydrate interaction, Pseudomonas aeruginosa PAO1*

INTRODUCTION

Pseudomonas aeruginosa is a rod shaped Gram-negative bacteria about 1−3 μm in length. Although common in the environment, it rarely causes disease in healthy humans. *P. aeruginosa* is usually linked to human disease, such as bacteremia in severe burn victims, chronic lung infection in cystic fibrosis (CF) patients, and acute ulcerative keratitis in soft contact lenses users.[1−3] Exotoxins and endotoxins released by *P. aeruginosa* can be life-threatening because they continue to damage host tissues even after the bacteria have been killed by antibiotics.[1] Bacterial adhesion to tissue surfaces is the initial step in *P. aeruginosa* infection.[4−6]

Adhesion of *P. aeruginosa* to mammalian cell surfaces is believed to be regulated by hydrophobic,[7−15] lectin−carbohydrate,[5,16−19] or antigen−antibody interactions.[3,20−22] Although all these interactions have been extensively studied individually to understand the mechanisms of microbial based pathogen infection,[7,16,19,22−24] only a few reports described bacterium−cell interactions in *P. aeruginosa* infection.[8,10,13] The glycoproteins presented on mammalian cell membranes have a certain degree of hydrophobicity[25] that can attract and interact with bacterial lectins.[16,26] Thus, bacterial adhesion to host tissues is regulated by both hydrophobic and lectin−carbohydrate interactions.

We compare hydrophobic and lectin−carbohydrate interactions on a quartz crystal microbalance with dissipation

Received: October 16, 2014
Accepted: December 30, 2014
Published: December 30, 2014

DOI: 10.1021/am508792k
ACS Appl. Mater. Interfaces 2015, 7, 1652−1661

Scheme 1. One-Pot RAFT Synthesis of the Diblock Copolymer P(LAEMA-*b*-NIPAAm)

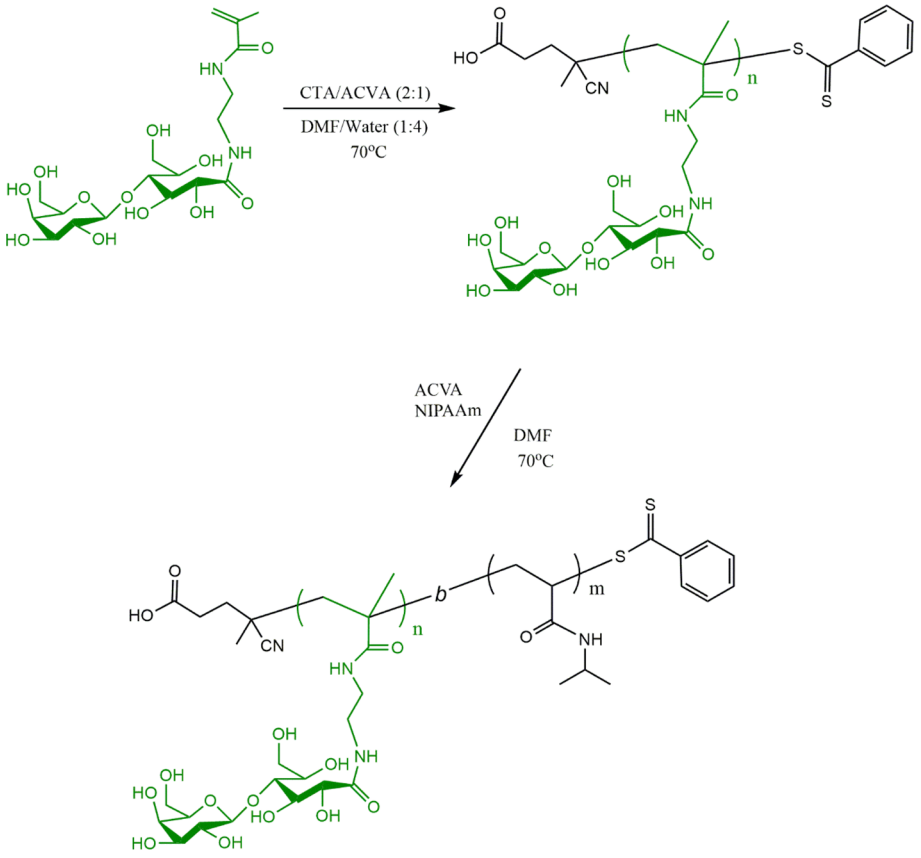

(QCM-D). Compared to other sensing techniques (e.g., surface plasmon resonance (SPR),[27] surface forces apparatus (SFA),[22] mass spectrometry (MS),[28] and atomic force microscopy (AFM)[29]), the QCM-D with flow modules can simulate the physiological conditions and provides a dynamic view on bacterial adhesion to a surface. Moreover, this technique provides the ability to probe the changes in softness (energy dissipation) and enables a better understanding on the bacterial adhesion process.[24,30,31] In the present study, the QCM-D sensor surface was therefore coated with three different types of polymers, namely, glyco-homopolymers, NIPAAm homopolymer, and their corresponding diblock copolymers (containing only a small amount of pendant carbohydrate residues). The diblock copolymers were synthesized by a one-pot reversible addition−fragmentation chain transfer (RAFT) polymerization[32] and directly immobilized on gold-coated QCM-D sensors.[24,33] By comparing *P. aeruginosa* PAO1 adhesion on different thermally responsive surfaces at different temperatures (20 and 37 °C), it was found that the lectin−carbohydrate interactions played a prominent role in bacterial adhesion besides hydrophobicity of the surfaces.

MATERIALS AND METHODS

Materials. Chemicals were purchased from Sigma-Aldrich Chemicals (Oakville, ON, Canada), and organic solvents were from Caledon Laboratories Ltd. (Georgetown, ON, Canada). The chain transfer agent 4-cyanopentanoic acid dithiobenzoate (CTP) and monomers were synthesized as previously described.[34−37]

Methods. Monomer structures and RAFT agent are shown in Scheme S1, Supporting Information. Average molecular weight (M_n) and polydispersity (M_w/M_n) were determined by gel permeation chromatography (GPC) using Pullulan standards (M_w = 5900−788 000 g mol^{-1}) at room temperature and a Viscotek model 250 dual detector [refractometer/viscometer in aqueous eluents (0.5 M sodium acetate and 0.5 M acetic acid, for glyco-homopolymers) or in 10 mM lithium bromide *N*,*N*′-dimethylformamide (DMF) solution (for the thermally responsive polymers)] with flow rate of 1.0 mL/min. Bacterium−polymer interactions were studied with a QCM-D (Q-Sense, Sweden, E4 chamber) using gold-coated sensor chips (frequency: 4.95 MHz, 50 kHz; cut: AT; diameter: 14 mm; thickness: 0.3 mm; surface roughness <3 nm (RMS); electrode layer: 10−300 nm). The numbers of bacteria adhering to sensor surfaces were visualized by fluorescence microscopy (Microscope Axio Imager.M2, Carl Zeiss, Germany) with a wide-field fluorescence microscope excitation light source (X-cite 120Q, Lumen Dynamic, ON, Canada).

RAFT polymerization was chosen to prepare well-defined glycopolymers.[35,37] In a typical polymerization of the homopolymers, 2-lactobionamidoethyl methacrylamide (LAEMA) (1 g, 2 mmol) was dissolved in 6 mL of distilled water in a 10 mL Schlenk tube with 1 mL of CTP (16 mg, 0. 057 mmol) and 4,4′-azobis (4-cyanovaleric acid) (ACVA) (8 mg, 0.032 mmol) in DMF stock solution. The tube was then sealed and degassed by purging it with nitrogen for 30 min. Polymerization was conducted in an oil bath (70 °C) for 24 h, followed by precipitation in acetone and subsequent washing with methanol to remove the unreacted monomers and residual RAFT agents. Polymerization was determined by Varian 500 ^{1}H NMR using D_2O. Polymer molecular weight and polydispersity were determined by aqueous gel permeation chromatography (GPC) (Viscotek GPC system) at room temperature with a flow rate of 1.0 mL/min.

One-Pot RAFT Synthesis of the Diblock Glycol-Copolymers. Diblock glycol-copolymers were prepared by one-pot RAFT synthesis in a water-DMF solution.[32] In a typical protocol on P(LAEMA-*b*-NIPAAm) synthesis, in a 10 mL Schlenk tube, LAEMA (134.2 mg, 0.29 mmol) was dissolved in 2 mL of double distilled deionized water before the addition of CTP (20 mg, 0.072 mmol) and ACVA (10 mg, 0.040 mmol) in DMF stock solution (0.5 mL). After degassing under nitrogen atmosphere for 30 min, the flask was placed in a preheated oil

DOI: 10.1021/am508792k
ACS Appl. Mater. Interfaces 2015, 7, 1652−1661

Table 1. Molecular Weight (M_n), Glycopolymer Content (φ), PDI (M_w/M_n), and Interactions with Bacterial Cells of Polymers Synthesized by RAFT

				bacterium−polymer interactions	
polymer[a]	φ (%)	M_n (GPC, g/mol)	M_w/M_n	20 °C	37 °C
P(GAPMA$_{39}$)	100	12 490	1.33	weak protein−carbohydrate interaction	weak protein−carbohydrate interaction
P(LAEMA$_{28}$)	100	13 338	1.30	strong protein−carbohydrate interaction	strong protein−carbohydrate interaction
P(NIPAAm$_{40}$)	0	4546	1.58	weak hydrophobic interaction	strong hydrophobic interaction
P(LAEMA$_2$-*b*-NIPAAm$_{40}$)	4	5656	1.31	weak hydrophobic interaction	strong protein−carbohydrate and hydrophobic interactions
P(GAPMA$_2$-*b*-NIPAAm$_{46}$)	4	6119	1.38	weak hydrophobic interaction	weak protein−carbohydrate and strong hydrophobic interactions

[a]P(GAPMA): glucose-derived glycopolymer; P(LAEMA): galactose-derived glycopolymer.

bath (70 °C) for 4 h, followed by the addition of 14 mL of degassed NIPAAm (1.142 g, 10.10 mmol) and ACVA (10 mg, 0.040 mmol) in DMF. The mixture was continuously agitated at 70 °C for 24 h and then purified by dialysis against double distilled deionized water for 3 days to remove any unreacted monomers and RAFT agents (Scheme 1). After the polymers were obtained by freeze-drying, the conversion and composition of the copolymer were determined by Varian 500 ^{1}H NMR in D_2O. Polymer molecular weight and molecular weight distribution were determined by DMF GPC (Viscotek GPC system) at room temperature with a flow rate of 1.0 mL/min.[36]

Polymer Lower Critical Solution Temperature Measurements. Polymer lower critical solution temperatures (LCSTs) were determined from 50% transmittance of the 0.1 w/v% synthesized NIPAAm based polymers in aqueous solution at 500 nm with a heating rate of 0.5 °C/min with a UV−vis spectrometer.

Bacterial Cultivation. *P. aeruginosa* PAO1 was streaked onto a Luria−Bertani (LB) agar plate and incubated at 37 °C overnight. A single colony was transferred into 5 mL of LB broth and grown overnight in a shaker incubator at 200 rpm and 37 °C. Stationary-phase hydrophobic bacterial cells with maximal lectin activity[38,39] were harvested by centrifugation at 4000*g* and 4 °C for 5 min. After decanting the supernatant, the pellets were resuspended in a 10 mM $CaCl_2$ solution. The centrifugation (4000*g*, 5 min) and resuspension procedure was repeated twice to remove traces of growth media and suspended extracellular polymeric substances from the solution.[40]

Studying the Bacteria−Polymer Interactions by QCM-D. Bacteria−polymer interactions were studied on a gold-coated QCM-D. Polymer aqueous solutions (1 mg/mL) were pumped into the sensor chambers at 20 °C with a flow rate of 50 μL/min to modify the gold-coated QCM-D sensor. When the frequency shifts were stable in the QCM-D (indicating that the polymer adsorption on the sensor surface was complete), the sensor surfaces were washed with DI water and then 10 mM $CaCl_2$ (0.15 mL/min) to remove weakly bound polymers from the surfaces. The bacterial suspension (10^7cells/mL) in 10 mM $CaCl_2$ was injected into the sensor chambers at 20 or 37 °C with a flow rate of 50 μL/min until the resonant frequencies of the sensors became stable.

Bacterial numbers on QCM-D sensor surfaces were counted with a fluorescent microscope (Microscope Axio Imager.M2, Carl Zeiss, Germany); for bacterial adhesion studied at 37 °C, temperature was controlled at 37 °C during the cell counting to avoid cell release from the thermal sensitive polymer surfaces.[41] All measurements were performed in duplicate with separately cultured bacteria.

After QCM-D measurement, bandwidths (Γ) were calculated using $\Gamma = Df/2$, where D is the dissipation shift measured by QCM-D and f is the frequency at each overtone (i.e., 5, 15, 25, 35, and 45 MHz at the fundamental frequency, third, fifth, seventh, and ninth overtone, respectively). The normalized shifts in frequency (Δf) and bandwidth ($\Delta\Gamma$) with the number of bacteria per unit area ($\Delta f/N_b$ and $\Delta\Gamma/N_b$) were then analyzed by small loading approximation. The small-loading approximation is an essential concept of QCM-D analysis, which includes the well-known formalism of QCM data analysis for planar layer systems (i.e., the Sauerbrey equation). The relationship is given as

$$\frac{\Delta f^*}{N_b} = \frac{\Delta f + i\Delta\Gamma}{N_b} = \frac{f_F}{N_b \pi Z_q} f_{osc} \frac{m\omega(k + i\omega\zeta)}{m\omega^2 - (k + i\omega\zeta)'}$$

where f_F is the fundamental frequency (5 MHz), Z_q is the acoustic impedance of AT-cut quartz crystal (8.8×10^6 kg/m^2/s), k is the spring constant, and f_{osc} is the oscillator strength ($0 < f_{osc} < 1$). When bacterial cells interact with a sensor surface strongly ($k \gg m\omega^2$, $\Delta f^* = (-2f_F/Z_q) f_{osc} \Delta m$), they can move together with the resonator and can be termed as inertial loading in the Sauerbrey sense. For weak elastic bonding ($k \ll m\omega^2$), the frequency shift is positive and the equation can be rewritten as $\Delta f^* = (f_F/\pi Z_q) f_{osc}(k/\omega)$, describing elastic loading.

The circular relation between the shifts in bandwidth and frequency, $\Delta\Gamma/N_b$ and $\Delta f/N_b$, respectively, can be plotted on a polar diagram with radii proportional to the adhesive bond stiffness k:

$$2R \approx \frac{\Delta\Gamma(\omega = \omega_b)}{N_b} \approx \frac{f_F}{N_b \pi Z_q} f_{osc} \frac{m\omega_b(\omega_b^2 + i\omega_b\gamma)}{i\omega_b\gamma} \approx \frac{f_F}{N_b \pi Z_q} \frac{k}{\gamma'}$$

where γ is the introduced damping rate, as the ratio of the drag coefficient (ξ) and the mass of the particle (m), with the dimension of frequency.[24,30,31,42,43] The radius of the circles in polar diagrams representing bacterial adhesion on different surfaces were then calculated in MATLAB with the Taubin method.

RESULTS AND DISCUSSION

Characterization of Thermally Responsive Diblock Copolymers. Glyco-homopolymers, NIPAAm homopolymer, and their corresponding thermally responsive diblock copolymers were synthesized by RAFT polymerization using dithiobenzoate as the RAFT agent. The RAFT process, which is applicable to a wide range of monomers under various conditions, enables one to control the polymer molecular weight and molecular weight distribution during the polymerization. Another advantage of RAFT polymerization is that the terminal dithioester groups can be used to directly interact with a gold surface[33] or can be reduced to thiol groups to introduce various functional groups.[44] RAFT polymerization was used here to have access to controlled telechelic polymer structures facilitating the interaction with the gold coated QCM-D surface.

Detailed characterization data of the synthesized polymers is shown in Table 1. The synthesized polymers showed relatively narrow molecular weight distributions. The copolymer compositions were determined by ^{1}H NMR (Figure S1, Supporting Information).

DOI: 10.1021/am508792k
ACS Appl. Mater. Interfaces 2015, 7, 1652−1661

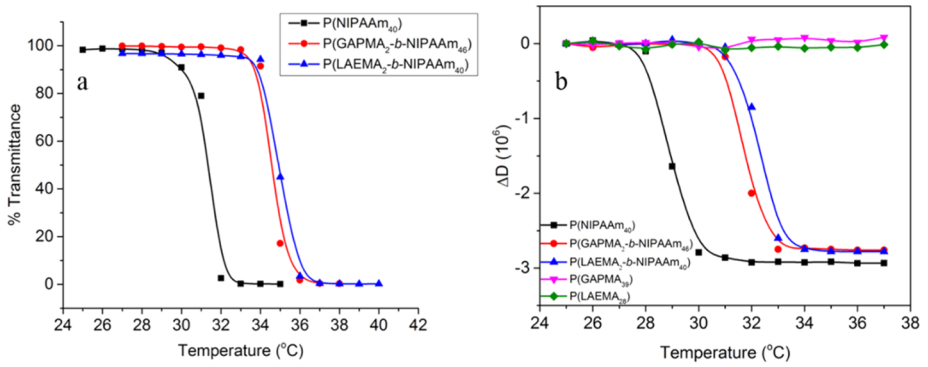

Figure 1. LCSTs of NIPAAm based polymers measured by (a) UV−vis and (b) QCM-D.

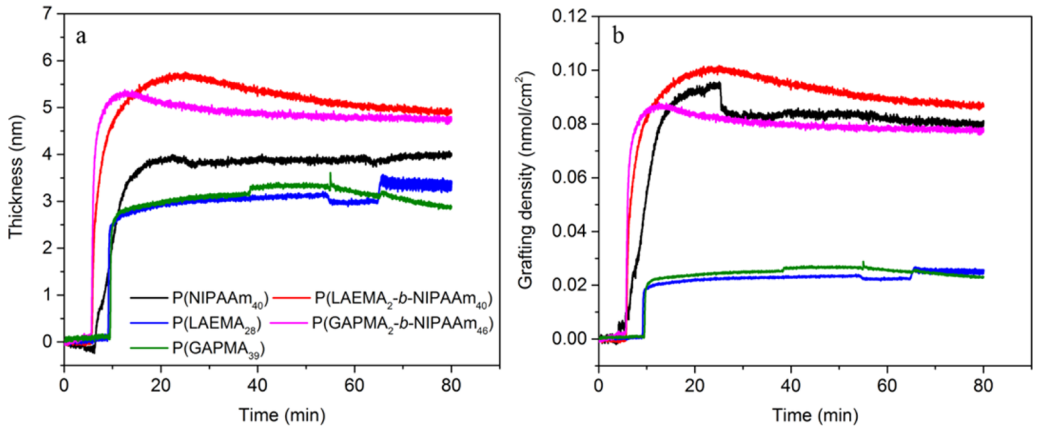

Figure 2. Thickness (a) and density (b) of polymer layers on QCM-D sensor surfaces.

LCSTs of NIPAAm based polymers are shown in Figure 1. The LCST of the NIPAAm homopolymer is around 32 °C, which agrees with the results from other reports.[45−48] However, in the case of the diblock copolymers, the LCSTs were found to increase to around 36 °C (Figure 1a), which conflicts with previous reports.[49,50] The hydrophilic pendent carbohydrate residues in the polymer chains may play an important role in this observation. In our current study, the carbohydrate residues can be considered as the end functional group of the polymer and, therefore, would be expected to decrease intermolecular aggregation[51] and hence cause an increase in LCST of the diblock copolymers. Although the carbohydrate repeating units presented in P(LAEMA$_2$-*b*-NIPAAm$_{40}$) and P(GAPMA$_2$-*b*-NIPAAm$_{46}$) were the same (Table 1), P-(LAEMA$_2$-*b*-NIPAAm$_{40}$) shows a slightly higher LCST (Figure 1a). The LCST of poly(*N*-isopropylacrylamide) [P(NIPAAm)] has been reported to be inversely dependent on the molecular weight of the polymer;[52,53] therefore, the difference in LCST between P(LAEMA$_2$-*b*-NIPAAm$_{40}$) and P(GAPMA$_2$-*b*-NI-PAAm$_{46}$) may be accounted for by the difference in molecular weight of the diblock copolymers (Table 1).

Although some studies claimed that, when the thermally responsive polymer was immobilized on a surface, its coil-to-globule transition temperature varied from its LCST in solution,[48] more recently, by measuring the thickness and contact angle changes of P(NIPAAm) brush in water as a function of temperature, Xue et al.[54] and Ko et al.[55] suggested that the polymer's coil-to-globule transition occurs at the temperature range of 23−32 °C and the polymer turns to its hydrophobic state at a temperature above the LCST. In this study, we also examine the P(NIPAAm) based polymers' coil-to-globule transition by QCM-D (Figure 1b). The results showed that, at a temperature range between 28 and 34 °C, the thermally responsive polymers (P(NIPAAm$_{40}$), P(LAEMA$_2$-*b*-NIPAAm$_{40}$), and P(GAPMA$_2$-*b*-NIPAAm$_{46}$)) undergo coil-to-globule transition, which results in the dissipation decreases due to the dehydration of the polymer chains.[48] This result shows a good correlation with the LCSTs measured by UV−vis (Figure 1a) and indicates that the thermally responsive polymers are either completely hydrophilic or hydrophobic when we compare the bacterial adhesion at 20 and 37 °C, respectively.

Polymer Modification of Gold-Coated QCM-D Sensor Surfaces. The polymers synthesized by RAFT polymerization were directly deposited on gold-coated QCM-D surfaces at 20 °C due to the strong interactions of the dithioester end terminal groups on the gold surface.[33] The thickness and density of the polymer layer on the QCM-D sensor surface were calculated using the Sauerbrey function provided by QTools as shown in Figure 2. All polymers were successfully immobilized on gold-coated QCM-D surfaces and generated polymer films with the thickness in a range of 3 to 5 nm (Figure 2a), which is comparable to the result from other researchers.[56] Since we are using the "grafting to" technique to anchor polymers on the gold-coated QCM-D sensor surface, the polymer film thickness is around half of the theoretical chain length values due to the polymers mushroom-like configuration at the sensor surface.[48] The polymers grafting density ranges from 0.02 to 0.09 nmol/cm^2 (Figure 2b). Compared to the results from Haddleton et al. that polymers with a dithio end group created less than 0.05 nmol/cm^2 surface coverage on a gold-coated QCM-D sensor surface,[33] the higher grafting density values that we obtained may be due to the shorter

DOI: 10.1021/am508792k
ACS Appl. Mater. Interfaces 2015, 7, 1652−1661

NIPAAm based polymers [P(NIPAAm$_{40}$), P(LAEMA$_2$-*b*-NIPAAm$_{40}$), and P(GAPMA$_2$-*b*-NIPAAm$_{46}$)] used. As expected, the glycopolymers [P(GAPMA$_{39}$) and P(LAEMA$_{28}$)] showed lower grafting densities possibly due to their higher molecular weights and molecular crowding on the sensor surface.[28]

***P. aeruginosa* PAO1 Adhesion to QCM-D Sensor Surfaces Varied with Different Polymer Modifications.** Although *P. aeruginosa* PAO1 surface properties (e.g., LPS[57] and lectin[58] expression) may vary at different temperatures, and thereby affect bacterial adhesion,[59] previous studies suggested that *P. aeruginosa* adhesion on both hydrophilic (glass or poly(ethylene oxide) (PEO))[60] and hydrophobic (polystyrene)[61] surfaces can be barely affected within the temperature range of 20 and 37 °C. Therefore, in the present study, the effect of temperature in bacterial adhesion on thermally responsive polymers modified sensor surfaces is expected to be minimal.

The numbers of *P. aeruginosa* PAO1 adhesion to different polymer modified surfaces at 20 and 37 °C are shown in Figure 3. Compared to bacterial adhesion on glycopolymer modified surfaces, a significantly ($p < 0.05$) smaller amount of *P. aeruginosa* PAO1 is observed from a carbohydrate-free P(NIPAAm$_{40}$) surface when temperature is controlled at 20 °C. Interestingly, although there are no glucose specific binding lectins present on the *P. aeruginosa* PAO1 membrane,[18,24] the bacteria can still interact with the P(GAPMA$_{39}$) surface and show a larger amount of cells adhered on the surface as compared to the galactose containing P(LAEMA$_{28}$) one. This observation might relate to the *P. aeruginosa* PAO1 cells interaction by their glucose transporters,[62,63] and the differences on bacterial cells adhesion on P(GAPMA$_{39}$) and P(LAEMA$_{28}$) surfaces might be explained by the "glycoside cluster effect".[64−67] On the other hand, an increase of the temperature from 20 to 37 °C seems to have negligible effect on *P. aeruginosa* PAO1 on P(LAEMA$_{28}$) and P(GAPMA$_{39}$) surfaces ($p = 0.97$, Figure 3); however, a significantly higher amount of bacterial cells could be found on the thermally responsive polymers surface [P(NIPAAm$_{40}$), P(LAEMA$_2$-*b*-NIPAAm$_{40}$), and P(GAPMA$_2$-*b*-NIPAAm$_{46}$)] as compared to the study performed at 20 °C (Figure 3). These observations can be explained as follows, at a temperature above the thermally responsive polymers LCST, the QCM-D surfaces become more hydrophobic, which would promote the bacterial adhesion.[41]

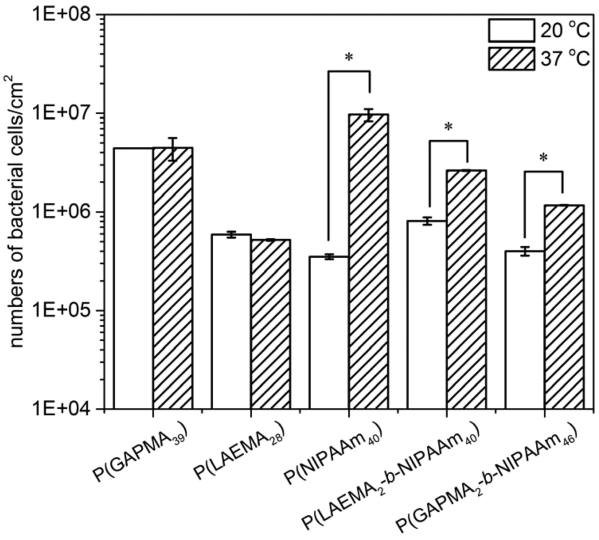

Figure 3. Numbers of *P. aeruginosa* PAO1 adhering to different polymer modified QCM-D surfaces at different temperatures. Values are presented as the mean ± SD ($n = 3$). The "asterisk" indicates significant differences ($p < 0.05$) on numbers of bacterial cells adhering on a surface at different temperatures.

Different bacterium−substratum interactions are also determined by QCM-D. At 20 and 37 °C, *P. aeruginosa* PAO1 adhesion to different polymer modified surfaces resulted in positive frequency shifts (Figures S2 and S3, Supporting Information), which indicated that the bacteria linked elastically to the polymer surfaces.[13,24,30,43] The frequency and bandwidth shifts were normalized with numbers of bacteria (Figure 3) on each QCM-D sensor ($\Delta F/N_b$ and $\Delta\Gamma/N_b$, respectively), and the bacterium bond stiffness on different polymer surfaces were quantitatively analyzed by comparing the diameters of the circles in the polar diagrams (Figure 4).[30,42]

Figure 4 shows the polar diagrams of *P. aeruginosa* PAO1 adhering to different polymer surfaces at 20 and 37 °C. The largest radius ($R_{P(LAEMA28)}$ = 294.93 μHz cm^2) in the polar diagram for *P. aeruginosa* PAO1 adhering to a P(LAEMA$_{28}$) modified QCM-D sensor surface at 20 °C in Figure 4a indicates a high bacterium−polymer bond stiffness,[24,30,42] which is probably due to the specific ligand−receptor interactions between galactose moieties on the glycopolymer backbones[37] and lectin (PA-IL) moieties on the bacterial membranes.[18,24] Although higher numbers of *P. aeruginosa* PAO1 were observed on the glucose-derived P(GAPMA$_{39}$)[36] modified surface as compared to the galactose based glycopolymer [P(LAEMA$_{28}$)] surface (Figure 3), the bacterial adhesion on the P(GAPMA$_{39}$) surface was found to be less elastic and showed a smaller radius in the polar diagrams ($R_{P(GAPMA39)}$ = 135.48 μHz cm^2, Figure 4a) as compared to the bacterial adhesion event on the P(LAEMA$_{28}$) surface,[24] and this could be due to the fact that there are no glucose specific binding lectins on the *P. aeruginosa* PAO1 membrane.[17]

Interestingly, the radius for bacterial adhesion to the P(LAEMA$_2$-*b*-NIPAAm$_{40}$) modified surface ($R_{P(LAEMA2\text{-}b\text{-}NIPAAm40)}$ = 66.89 μHz cm^2) at 20 °C was found to be much smaller than $R_{P(LAEMA28)}$ but closer to that on the P(NIPAAm$_{40}$) modified surface ($R_{P(NIPAAm40)}$ = 45.29 μHz cm^2) (Figure 4a). On the basis of the "glycoside cluster effect" which implies that multivalent saccharide ligands can improve the binding affinity of carbohydrate−lectin interactions,[64−67] the above observation may be due to the number of galactose residues accessible on the P(LAEMA$_2$-*b*-NIPAAm$_{40}$) modified sensor surface. At 20 °C, P(LAEMA$_2$-*b*-NIPAAm$_{40}$) chains on the sensor surface are more hydrophilic, and hence, due to the random coil conformation of the chains, some of the carbohydrate residues may be buried within the polymer chains and may not be accessible on the surface to interact with the *P. aeruginosa* PAO1 membrane (Scheme 2).[41,49,68,69] Therefore, in this condition, *P. aeruginosa* PAO1 adhesion to P(LAEMA$_2$-*b*-NIPAAm$_{40}$) modified sensor surfaces was similar to that on P(NIPAAm$_{40}$) surfaces, providing the stiffness values presented in Figure 4a.

At 37 °C, the $R_{P(GAPMA39)}$ value for bacterial adhesion to the P(GAPMA$_{39}$) modified surface is 136.49 μHz cm^2 (black circle, Figure 4c), which is close to the result obtained on the same surface at 20 °C (135.48 μHz cm^2, black circle in Figure 4a). Interestingly, for the P(LAEMA$_{28}$) modified surface, the

DOI: 10.1021/am508792k
ACS Appl. Mater. Interfaces 2015, 7, 1652−1661

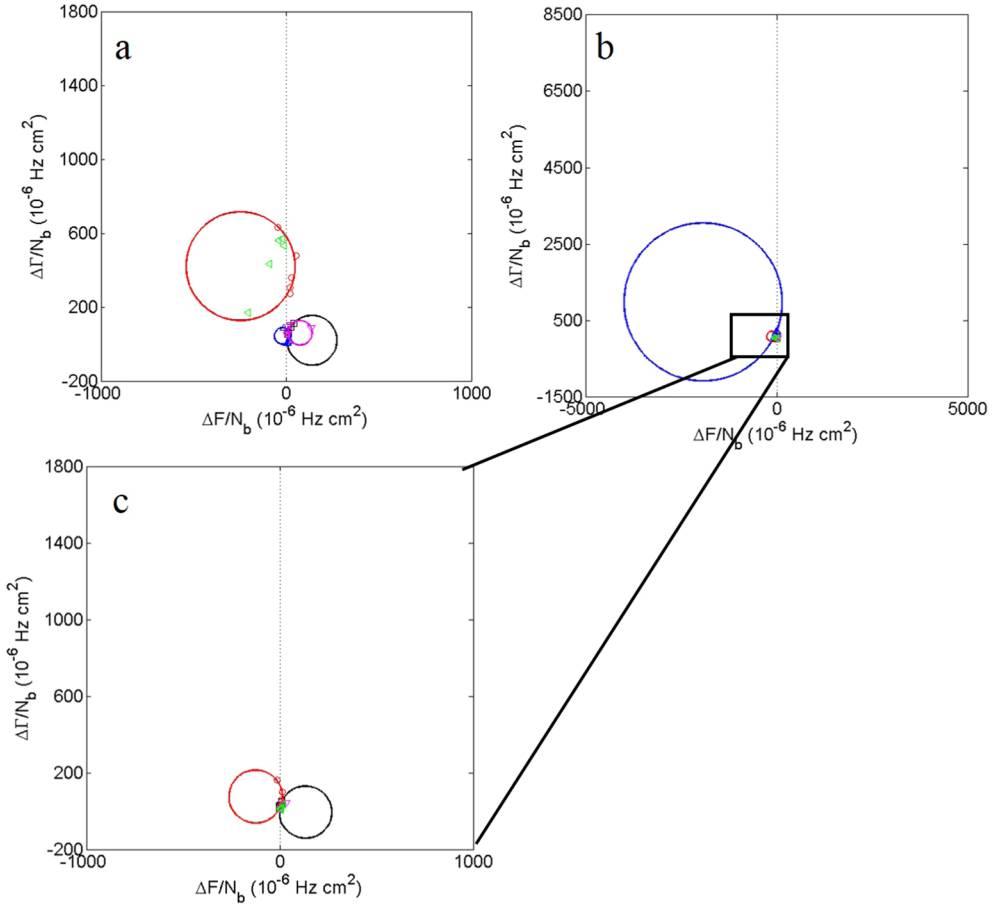

Figure 4. Polar diagrams of bandwidth and frequency shifts for (a) *P. aeruginosa* PAO1 adhesion to different polymer surfaces at 20 °C [$R_{P(LAEMA28)}$ > $R_{P(GAPMA39)}$ > $R_{P(LAEMA2\text{-}b\text{-}NIPAAm40)}$ > $R_{P(NIPAAm40)}$], (b) *P. aeruginosa* PAO1 adhesion to different polymer surfaces at 37 °C [$R_{P(NIPAAm40)} \gg R_{P(GAPMA39)} \approx R_{P(LAEMA28)}$)], and (c) *P. aeruginosa* PAO1 adhesion to glycopolymers surfaces at 37 °C. [black: P(GAPMA$_{39}$); red: P(LAEMA$_{28}$); blue: P(NIPAAm$_{40}$); pink: P(LAEMA$_2$-*b*-NIPAAm$_{40}$); green: P(GAPMA$_2$-*b*-NIPAAm$_{46}$)].

Scheme 2. Schematic Representation of *P. aeruginosa* PAO1 Adhesion on a Thermally Responsive P(LAEMA$_2$-*b*-NIPAAm$_{40}$) Modified QCM-D Sensor Surface at Different Temperatures

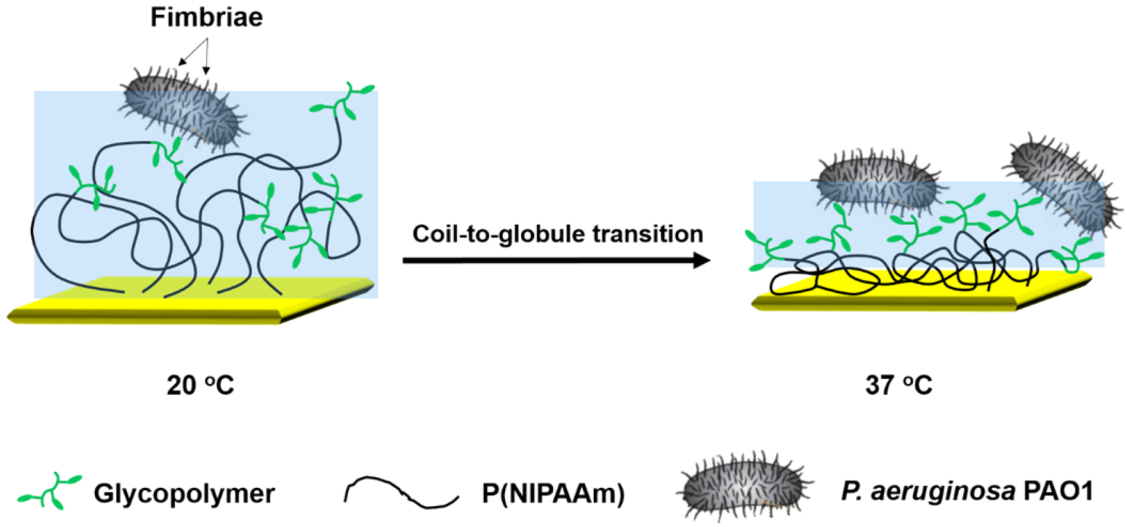

$R_{P(LAEMA28)}$ value was reduced to 138.61 μHz cm^2 at 37 °C (pink circle, Figure 4c) as compared to the one obtained for bacterial adhesion on the same surface at 20 °C (294.93 μHz cm^2). This could be due to the decrease in binding affinity of the PA-IL to galactose residues as the temperature was increased from 20 to 37 °C.[50]

Both the numbers of *P. aeruginosa* PAO1 (Figures 3 and 5) and the radii in polar diagrams ($R_{P(NIPAAm40)}$ = 2073.40 μHz cm^2, Figure 4b) for bacterial adhesion on the P(NIPAAm$_{40}$)

DOI: 10.1021/am508792k
ACS Appl. Mater. Interfaces 2015, 7, 1652−1661

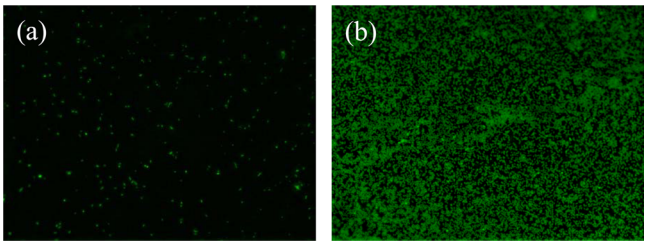

Figure 5. *P. aeruginosa* PAO1 adhesion to a P(NIPAAm$_{40}$) modified sensor surface at different temperatures (a: 20 °C; b: 37 °C).

surface were found to increase significantly at 37 °C. These results showed a stronger bacterium−substratum bond stiffness formed on the P(NIPAAm$_{40}$) modified surface at 37 °C indicative of the hydrophobic nature of the P(NIPAAM) where the temperature is above the LCST.[46,47] However, this may not be a valid explanation due to the aggregation of the *P. aeruginosa* PAO1 cells on the P(NIPAAm$_{40}$) modified surface at 37 °C making the cell counting difficult, and hence, the bond stiffness predicted in the polar diagrams may be incorrect (Figure 5). In addition, it was not possible to determine the bond stiffness involved in bacterial adhesion to P(LAEMA$_2$-*b*-NIPAAm$_{40}$) and P(GAPMA$_2$-*b*-NIPAAm$_{46}$) surfaces using the coupled resonance model, as the frequency shifts were positive at all overtones (Figure S3, Supporting Information) and no zero crossing frequencies could be observed from the polar diagrams (Figure 4c).[31] To address these issues and compare *P. aeruginosa* PAO1 adhesion to different polymer surfaces at 37 °C, $\Delta F/\Delta D$ values were instead used to cancel out the effect of bacterial numbers in the bacterium−substratum connection analysis. A higher $\Delta F/\Delta D$ value is usually associated with a stronger elastic connection.[13]

The $\Delta F/\Delta D$ values of *P. aeruginosa* PAO1 adhesion to different polymer surfaces at 20 and 37 °C are shown in Figure 6a,b, respectively. The values for bacterial adhesion to different polymer surfaces at 20 °C (Figure 6a) and the P(LAEMA$_{28}$) surface at 37 °C (Figure 6b) showed good agreement with the results from the polar diagrams (Figure 4a,c). Interestingly, although bacterial adhesion to the P(GAPMA$_{39}$) modified surface showed a similar bond stiffness at different temperatures in the polar diagrams (Figure 4a,c), $\Delta F/\Delta D$ values calculated at different temperatures gave different results. At low overtones, $\Delta F/\Delta D$ values for bacterial adhesion to the P(GAPMA$_{39}$) surface were positive at 37 °C but became less positive at higher overtones ($n > 5$) (Figure 6b). This behavior may be due to the increasing flexibility of bacterium−polymer chains at higher temperature. Negative $\Delta F/\Delta D$ values at high overtones are due to the viscous takeover as this is the predominant factor in the viscoelastic bacterium−substratum connection.[13]

Interestingly, at 37 °C, although bacterial adhesion to the P(NIPAAm$_{40}$) modified surface showed the highest bond stiffness in the polar diagrams (Figure 4b), this result was not in agreement to the data shown in Figure 6b. The lowest $\Delta F/\Delta D$ values obtained for *P. aeruginosa* PAO1 adhesion to the P(NIPAAm$_{40}$) modified surface at 37 °C suggested that the bacterium interacted weakly with the hydrophobic P(NIPAAm$_{40}$) surface. As bacterial cells aggregated on the P(NIPAAm$_{40}$) surface at 37 °C (Figure 5), an increase in dissipation was observed, possibly due to the large amount of water entrapped between bacterial cells or by viscous friction at the liquid gaps on bacterium−bacterium and bacterium−substratum interfaces.[13] The highest $\Delta F/\Delta D$ values were observed when bacterial adhered on the P(LAEMA$_2$-*b*-NIPAAm$_{40}$) surface at 37 °C. Since the thermally responsive glycopolymer (P(LAEMA$_2$-*b*-NIPAAm$_{40}$)) turned to its hydrophobic state and exposed more carbohydrate residues (galactose) during the coil-to-globular transition at a temperature higher than its LCST, an enhanced *P. aeruginosa* PAO1 adhesion on the P(LAEMA$_2$-*b*-NIPAAm$_{40}$) surface was noted to be possibly driven by both hydrophobic[14] and lectin−carbohydrate interactions (Scheme 2).[24]

To further illustrate the role of lectin−carbohydrate and hydrophobic interactions in bacterial adhesion on the surface, we performed a competitive assay, in which the interaction between galactophilic lectin (PA-IL) and galactose containing glycopolymers was competitively blocked by the addition of an excess of galactose containing compound (lactobionic acid) into the bacterial suspension. The $\Delta F/\Delta D$ values of *P. aeruginosa* PAO1 adhesion to different polymer surfaces in the presence of lactobionic acid at 20 and 37 °C are shown in Figure 7a,b, respectively.

Compared to the bacterial adhesion to galactose containing glycopolymer surfaces [P(LAEMA$_{28}$) and P(LAEMA$_2$-*b*-NIPAAm$_{40}$)] at 20 °C (Figure 6a), the $\Delta F/\Delta D$ values shifted to negative values when lactobionic acid was added in the bacterial suspension (Figure 7a), indicating contact between bacterium and carbohydrate substratum has changed from elastic to a weaker viscous connection (Figure 7d). These changes might relate to the blocking of the interaction between the bacterial galactophilic PA-IL and galactose containing glycopolymers, as the numbers of *P. aeruginosa* PAO1 on P(LAEMA$_{28}$) and P(LAEMA$_2$-*b*-NIPAAm$_{40}$) surfaces are reduced significantly in lactobionic acid solution at 20 °C (Figures 7c and S4, Supporting Information). On the other hand, compared to *P. aeruginosa* PAO1 adhesion on polymer

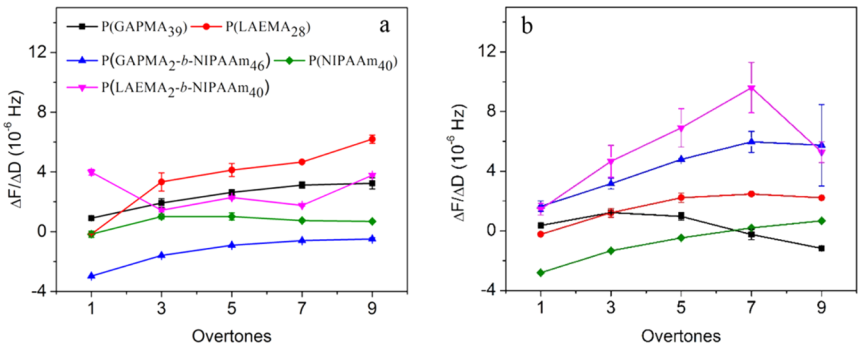

Figure 6. $\Delta F/\Delta D$ values calculated at the end of *P. aeruginosa* PAO1 adhesion to different surfaces. (a) 20 °C; (b) 37 °C.

DOI: 10.1021/am508792k
ACS Appl. Mater. Interfaces 2015, 7, 1652−1661

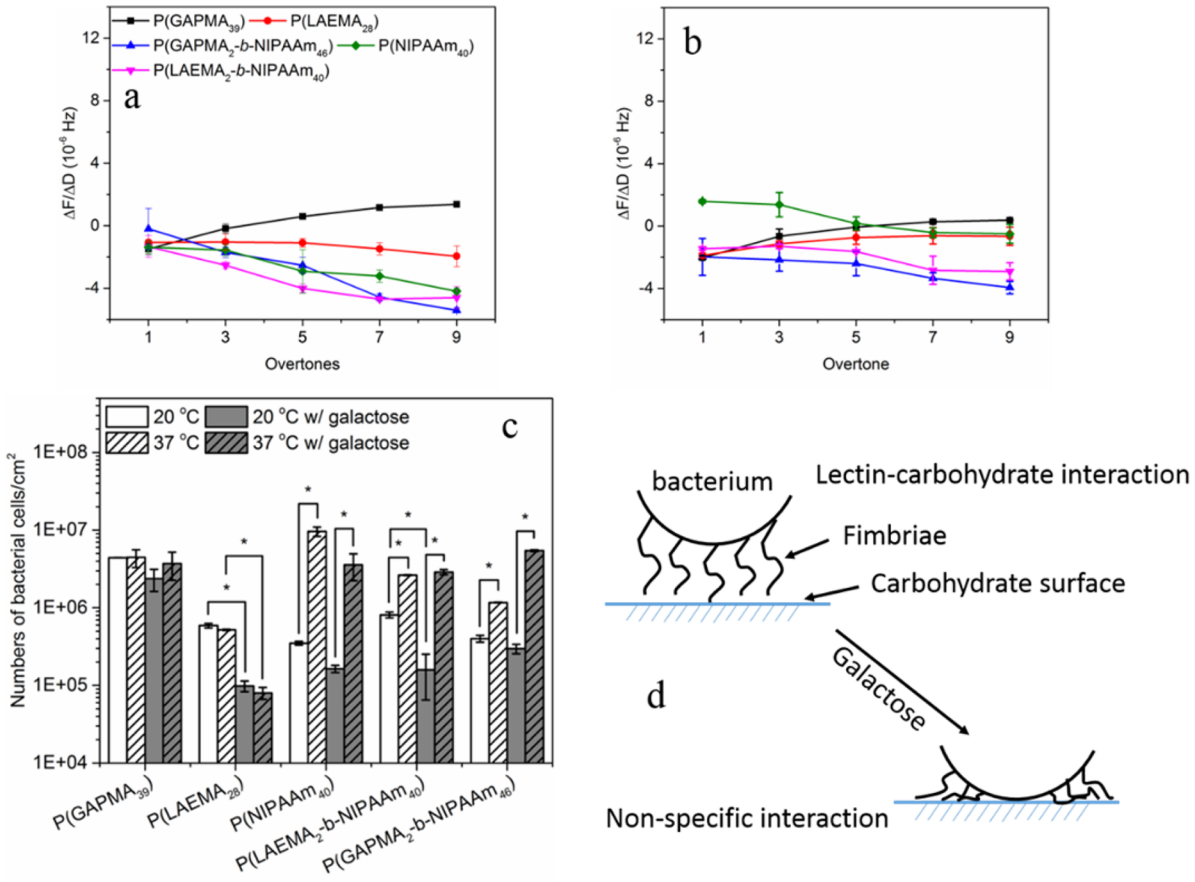

Figure 7. $\Delta F/\Delta D$ values calculated when *P. aeruginosa* PAO1 adheres to different surfaces in the presence of lactobionic acid. (a) 20 °C; (b) 37 °C. (c) Numbers of *P. aeruginosa* PAO1 adhering to different polymer modified QCM-D surfaces at different temperatures. The "asterisk" indicates significant differences ($p < 0.05$) on numbers of bacterial cells adhering on a surface at different temperatures. Values are presented as the mean ± SD ($n = 3$). (d) Schematic illustration of nonspecific and lectin−carbohydrate based bacterium−substratum interactions.

surfaces in 10 mM Ca^{2+} (Figures 3 and 6a), neither bacterium−substratum interaction (Figure 7a) nor numbers of bacterial cells (Figure 7c) on P($GAPMA_{39}$), P($GAPMA_2$-*b*-$NIPAAm_{46}$), and P($NIPAAm_{40}$) surfaces has been changed significantly in lactobionic acid solution. These observations might suggest that the addition of lactobionic acid only affects the lectin−carbohydrate interaction between *P. aeruginosa* PAO1 and galactose containing polymers.

At 37 °C, although the galactophilic PA-IL has been blocked by lactobionic acid, the numbers of *P. aeruginosa* PAO1 observed on the three thermally responsive polymer [P($NIPAAm_{40}$), P($GAPMA_2$-*b*-$NIPAAm_{46}$), and P($LAEMA_2$-*b*-$NIPAAm_{40}$)] surfaces are close (Figure 7c). The above observations might be due to the increased hydrophobicity of the surface enhancing the bacterium−substratum affinity. On the other hand, similar to bacterial adhesion to the P($LAEMA_{28}$) and P($LAEMA_2$-*b*-$NIPAAm_{40}$) surface at 20 °C (Figure 7a), the $\Delta F/\Delta D$ shifted to negative values at 37 °C when lactobionic acid was introduced to the bacterial suspension (Figure 7b). Interestingly, although no galactose is present on P($NIPAAm_{40}$) and P($GAPMA_2$-*b*-$NIPAAm_{46}$), in lactobionic acid solution, the $\Delta F/\Delta D$ values also change their signs at 37 °C (Figure 7b) as compared to the results obtained in 10 mM Ca^{2+} (Figure 6b). These results showed a very good agreement to Marcus et al.'s study[13] in which the hydrophilic *P. aeruginosa* PAO1 adhered to a surface. Therefore, when the negatively charged lactobionic acid ($pK_a = 3.8$) is bound to the galactophilic PA-IL on the *P. aeruginosa* PAO1 membrane, the bacterial surface become more hydrophilic so that more water would appear on the bacterium−substratum interface, which may alter the bacterium−substratum interaction or increase the viscous friction to make the $\Delta F/\Delta D$ values closer to zero (Figure 7b).

CONCLUSION

Well-defined thermally responsive glycopolymers carrying galactose residues as pendant groups were successfully synthesized by the one-pot RAFT process and subsequently immobilized on gold-coated QCM-D sensor surfaces. Interactions between the polymers and *P. aeruginosa* PAO1 were studied by QCM-D at 20 and 37 °C and analyzed by a coupled resonance model. Although a significantly higher number of *P. aeruginosa* PAO1 adhered to a hydrophobic surface [P($NIPAAm_{40}$)] at 37 °C than at 20 °C, the bond stiffness was much lower as compared to bacterial adhesion to glycopolymer homopolymers [P($LAEMA_{28}$) and P($GAPMA_{39}$)] and biomimetic cell surfaces [P($LAEMA_2$-*b*-$NIPAAm_{40}$) and P($GAPMA_2$-*b*-$NIPAAm_{46}$) modified sensor surfaces]. These results suggest that bacterial adhesion is regulated by specific lectin−carbohydrate interactions and is expected to be the dominant factor in pathogen infection.

DOI: 10.1021/am508792k
ACS Appl. Mater. Interfaces 2015, 7, 1652−1661

■ ASSOCIATED CONTENT

Supporting Information

^{1}H NMR spectra of P(LAEMA$_{28}$), P(NIPAAm$_{40}$), and P(LAEMA$_2$-*b*-NIPAAm$_{40}$) synthesized by the RAFT technique; frequency and dissipation shifts for *P. aeruginosa* PAO1 adhesion on different polymer treated QCM-D sensors at 20 and 37 °C. This material is available free of charge via the Internet at http://pubs.acs.org.

■ AUTHOR INFORMATION

Corresponding Authors

*E-mail: yang.liu@ualberta.ca (Y. Liu).
*E-mail: narain@ualberta.ca (R. Narain).

Notes

The authors declare no competing financial interest.

■ ACKNOWLEDGMENTS

This research was supported by research grants from the Natural Sciences and Engineering Research Council (NSERC) of Canada and the Canada Foundation for Innovation (CFI).

■ REFERENCES

(1) Campa, M., Bendinelli, M., Friedman, H., Eds. *Pseudomonas aeruginosa as an Opportunistic Pathogen*; Springer: New York, 1993.
(2) Lyczak, J. B.; Cannon, C. L.; Pier, G. B. Establishment of *Pseudomonas aeruginosa* Infection: Lessons from a Versatile Opportunist. *Microbes Infect.* **2000**, *2*, 1051−1060.
(3) Pier, G. B. *Pseudomonas* and Related Gram-Negative Bacillary Infections. In *Goldman's Cecil Medicine*, Twenty-Fourth ed.; W.B. Saunders: Philadelphia, 2012.
(4) Larrosa, M.; Truchado, P.; Espín, J. C.; Tomás-Barberán, F. A.; Allende, A.; García-Conesa, M. T. Evaluation of *Pseudomonas aeruginosa* (PAO1) Adhesion to Human Alveolar Epithelial Cells A549 Using SYTO 9 Dye. *Mol. Cell. Probes* **2012**, *26*, 121−126.
(5) Doig, P.; Todd, T.; Sastry, P. A.; Lee, K. K.; Hodges, R. S.; Paranchych, W.; Irvin, R. T. Role of Pili in Adhesion of *Pseudomonas aeruginosa* to Human Respiratory Epithelial Cells. *Infect. Immun.* **1988**, *56*, 1641−1646.
(6) Maddikeri, R. R.; Tosatti, S.; Schuler, M.; Chessari, S.; Textor, M.; Richards, R. G.; Harris, L. G. Reduced Medical Infection Related Bacterial Strains Adhesion on Bioactive RGD Modified Titanium Surfaces: A First Step Toward Cell Selective Surfaces. *J. Biomed. Mater. Res., Part A* **2008**, *84A*, 425−435.
(7) van Loosdrecht, M. C.; Lyklema, J.; Norde, W.; Schraa, G.; Zehnder, A. J. The Role of Bacterial Cell Wall Hydrophobicity in Adhesion. *Appl. Environ. Microbiol.* **1987**, *53*, 1893−1897.
(8) Busscher, H. J.; Weerkamp, A. H. Specific and Non-Specific Interactions in Bacterial Adhesion to Solid Substrata. *FEMS Microbiol. Lett.* **1987**, *46*, 165−173.
(9) Bos, R.; van der Mei, H. C.; Busscher, H. J. Physico-Chemistry of Initial Microbial Adhesive Interactions − Its Mechanisms and Methods for Study. *FEMS Microbiol. Rev.* **1999**, *23*, 179−230.
(10) Doyle, R. J. Contribution of The Hydrophobic Effect to Microbial Infection. *Microbes Infect.* **2000**, *2*, 391−400.
(11) Bruinsma, G. M.; van der Mei, H. C.; Busscher, H. J. Bacterial Adhesion to Surface Hydrophilic and Hydrophobic Contact Lenses. *Biomaterials* **2001**, *22*, 3217−3224.
(12) Karakecili, A. G.; Gumusderelioglu, M. Comparison of Bacterial and Tissue Cell Initial Adhesion on Hydrophilic/Hydrophobic Biomaterials. *J. Biomater. Sci., Polym. Ed.* **2002**, *13*, 185−196.
(13) Marcus, I. M.; Herzberg, M.; Walker, S. L.; Freger, V. *Pseudomonas aeruginosa* Attachment on QCM-D Sensors: The Role of Cell and Surface Hydrophobicities. *Langmuir* **2012**, *28*, 6396−6402.
(14) Hwang, G.; Liang, J.; Kang, S.; Tong, M.; Liu, Y. The Role of Conditioning Film Formation in *Pseudomonas aeruginosa* PAO1 Adhesion to Inert Surfaces in Aquatic Environments. *Biochem. Eng. J.* **2013**, *76*, 90−98.
(15) Hwang, G.; Kang, S.; El-Din, M. G.; Liu, Y. Impact of an Extracellular Polymeric Substance (EPS) Precoating on The Initial Adhesion of *Burkholderia cepacia* and *Pseudomonas aeruginosa*. *Biofouling* **2012**, *28*, 525−538.
(16) Sharon, N. Bacterial Lectins, Cell-Cell Recognition and Infectious Disease. *FEBS Lett.* **1987**, *217*, 145−157.
(17) Tielker, D.; Hacker, S.; Loris, R.; Strathmann, M.; Wingender, J.; Wilhelm, S.; Rosenau, F.; Jaeger, K.-E. *Pseudomonas aeruginosa* Lectin LecB Is Located in the Outer Membrane and Is Involved in Biofilm Formation. *Microbiology* **2005**, *151*, 1313−1323.
(18) Diggle, S. P.; Stacey, R. E.; Dodd, C.; Cámara, M.; Williams, P.; Winzer, K. The Galactophilic Lectin, LecA, Contributes to Biofilm Development in *Pseudomonas aeruginosa*. *Environ. Microbiol.* **2006**, *8*, 1095−1104.
(19) Shen, Z.; Huang, M.; Xiao, C.; Zhang, Y.; Zeng, X.; Wang, P. G. Nonlabeled Quartz Crystal Microbalance Biosensor for Bacterial Detection Using Carbohydrate and Lectin Recognitions. *Anal. Chem.* **2007**, *79*, 2312−2319.
(20) Pier, G. B. *Pseudomonas aeruginosa* Lipopolysaccharide: A Major Virulence Factor, Initiator of Inflammation and Target for Effective Immunity. *Int. J. Med. Microbiol.* **2007**, *297*, 277−295.
(21) Preston, M. J.; Berk, J. M.; Hazlett, L. D.; Berk, R. S. Serum Antibody Response to *Pseudomonas aeruginosa* Antigens During Corneal Infection. *Infect. Immun.* **1991**, *59*, 1984−1990.
(22) Lu, Q.; Wang, J.; Faghihnejad, A.; Zeng, H.; Liu, Y. Understanding the Molecular Interactions of Lipopolysaccharides During *E. coli* Initial Adhesion with a Surface Forces Apparatus. *Soft Matter* **2011**, *7*, 9366−9379.
(23) Su, X.-L.; Li, Y. A QCM Immunosensor for *Salmonella* Detection with Simultaneous Measurements of Resonant Frequency and Motional Resistance. *Biosens. Bioelectron.* **2005**, *21*, 840−848.
(24) Wang, Y.; Narain, R.; Liu, Y. Study of Bacterial Adhesion on Different Glycopolymer Surfaces by Quartz Crystal Microbalance with Dissipation. *Langmuir* **2014**, *30*, 7377−7387.
(25) Ghebeh, H.; Gillis, J.; Butler, M. Measurement of Hydrophobic Interactions of Mammalian Cells Grown in Culture. *J. Biotechnol.* **2002**, *95*, 39−48.
(26) Krogfelt, K. A.; Bergmans, H.; Klemm, P. Direct Evidence that the Fimh Protein is the Mannose-Specific Adhesin of *Escherichia-coli* Type-1 Fimbriae. *Infect. Immun.* **1990**, *58*, 1995−1998.
(27) Pranzetti, A.; Salaün, S.; Mieszkin, S.; Callow, M. E.; Callow, J. A.; Preece, J. A.; Mendes, P. M. Model Organic Surfaces to Probe Marine Bacterial Adhesion Kinetics by Surface Plasmon Resonance. *Adv. Funct. Mater.* **2012**, *22*, 3672−3681.
(28) Tseng, Y.-T.; Chang, H.-Y.; Huang, C.-C. A Mass Spectrometry-Based Immunosensor for Bacteria Using Antibody-Conjugated Gold Nanoparticles. *Chem. Commun.* **2012**, *48*, 8712−8714.
(29) Razatos, A.; Ong, Y.-L.; Sharma, M. M.; Georgiou, G. Molecular Determinants of Bacterial Adhesion Monitored by Atomic Force Microscopy. *Proc. Natl. Acad. Sci. U.S.A.* **1998**, *95*, 11059−11064.
(30) Olsson, A. L. J.; van der Mei, H. C.; Johannsmann, D.; Busscher, H. J.; Sharma, P. K. Probing Colloid-Substratum Contact Stiffness by Acoustic Sensing in a Liquid Phase. *Anal. Chem.* **2012**, *84*, 4504−4512.
(31) Olsson, A. L. J.; van der Mei, H. C.; Busscher, H. J.; Sharma, P. K. Novel Analysis of Bacterium-Substratum Bond Maturation Measured Using a Quartz Crystal Microbalance. *Langmuir* **2010**, *26*, 11113−11117.
(32) Chaduc, I.; Zhang, W.; Rieger, J.; Lansalot, M.; D'Agosto, F.; Charleux, B. Amphiphilic Block Copolymers from a Direct and One-Pot RAFT Synthesis in Water. *Macromol. Rapid Commun.* **2011**, *32*, 1270−1276.
(33) Slavin, S.; Soeriyadi, A. H.; Voorhaar, L.; Whittaker, M. R.; Becer, C. R.; Boyer, C.; Davis, T. P.; Haddleton, D. M. Adsorption Behaviour of Sulfur Containing Polymers to Gold Surfaces Using QCM-D. *Soft Matter* **2011**, *8*, 118−128.
(34) Benaglia, M.; Rizzardo, E.; Alberti, A.; Guerra, M. Searching for More Effective Agents and Conditions for the RAFT Polymerization

DOI: 10.1021/am508792k
ACS Appl. Mater. Interfaces 2015, 7, 1652−1661

of MMA: Influence of Dithioester Substituents, Solvent, and Temperature. *Macromolecules* **2005**, *38*, 3129−3140.
(35) Deng, Z.; Bouchékif, H.; Babooram, K.; Housni, A.; Choytun, N.; Narain, R. Facile Synthesis of Controlled-Structure Primary Amine-Based Methacrylamide Polymers via the Reversible Addition-Fragmentation Chain Tansfer Process. *J. Polym. Sci., Part A: Polym. Chem.* **2008**, *46*, 4984−4996.
(36) Deng, Z.; Ahmed, M.; Narain, R. Novel Well-Defined Glycopolymers Synthesized via the Reversible Addition Fragmentation Chain Transfer Process in Aqueous Media. *J. Polym. Sci., Part A: Polym. Chem.* **2009**, *47*, 614−627.
(37) Deng, Z.; Li, S.; Jiang, X.; Narain, R. Well-Defined Galactose-Containing Multi-Functional Copolymers and Glyconanoparticles for Biomolecular Recognition Processes. *Macromolecules* **2009**, *42*, 6393−6405.
(38) Rickard, A. H.; Leach, S. A.; Buswell, C. M.; High, N. J.; Handley, P. S. Coaggregation between Aquatic Bacteria Is Mediated by Specific-Growth-Phase-Dependent Lectin-Saccharide Interactions. *Appl. Environ. Microbiol.* **2000**, *66*, 431−434.
(39) Diggle, S. P.; Winzer, K.; Chhabra, S. R.; Worrall, K. E.; Cámara, M.; Williams, P. The *Pseudomonas aeruginosa* Quinolone Signal Molecule Overcomes the Cell Density-Dependency of the Quorum Sensing Hierarchy, Regulates Rhl-Dependent Genes at the Onset of Stationary Phase and Can Be Produced in the Absence of LasR. *Mol. Microbiol.* **2003**, *50*, 29−43.
(40) Sun, X.; Danumah, C.; Liu, Y.; Boluk, Y. Flocculation of Bacteria by Depletion Interactions Due to Rod-Shaped Cellulose Nanocrystals. *Chem. Eng. J.* **2012**, *198−199*, 476−481.
(41) Ebara, M.; Yamato, M.; Aoyagi, T.; Kikuchi, A.; Sakai, K.; Okano, T.; Novel, A. Approach to Observing Synergy Effects of PHSRN on Integrin-RGD Binding Using Intelligent Surfaces. *Adv. Mater.* **2008**, *20*, 3034−3038.
(42) Olsson, A. L. J.; Arun, N.; Kanger, J. S.; Busscher, H. J.; Ivanov, I. E.; Camesano, T. A.; Chen, Y.; Johannsmann, D.; van der Mei, H. C.; Sharma, P. K. The Influence of Ionic Strength on the Adhesive Bond Stiffness of Oral *Streptococci* Possessing Different Surface Appendages as Probed Using AFM and QCM-D. *Soft Matter* **2012**, *8*, 9870−9876.
(43) Reviakine, I.; Johannsmann, D.; Richter, R. P. Hearing What You Cannot See and Visualizing What You Hear: Interpreting Quartz Crystal Microbalance Data from Solvated Interfaces. *Anal. Chem.* **2011**, *83*, 8838−8848.
(44) Willcock, H.; O'Reilly, R. K. End Group Removal and Modification of RAFT Polymers. *Polym. Chem.* **2010**, *1*, 149−157.
(45) Barker, I. C.; Cowie, J. M. G.; Huckerby, T. N.; Shaw, D. A.; Soutar, I.; Swanson, L. Studies of the "Smart" Thermoresponsive Behavior of Copolymers of *N*-Isopropylacrylamide and *N*,*N*-Dimethylacrylamide in Dilute Aqueous Solution. *Macromolecules* **2003**, *36*, 7765−7770.
(46) Gil, E. S.; Hudson, S. M. Stimuli-Reponsive Polymers and Their Bioconjugates. *Prog. Polym. Sci.* **2004**, *29*, 1173−1222.
(47) Hoare, T.; Pelton, R. Engineering Glucose Swelling Responses in Poly(*N*-isopropylacrylamide)-Based Microgels. *Macromolecules* **2007**, *40*, 670−678.
(48) Zhang, G. Z. Study on Conformation Change of Thermally Sensitive Linear Grafted Poly(*N*-isopropylacrylamide) Chains by Quartz Crystal Microbalance. *Macromolecules* **2004**, *37*, 6553−6557.
(49) Idota, N.; Ebara, M.; Kotsuchibashi, Y.; Narain, R.; Aoyagi, T. Novel Temperature-Responsive Polymer Brushes with Carbohydrate Residues Facilitate Selective Adhesion and Collection of Hepatocytes. *Sci. Technol. Adv. Mater.* **2012**, *13*, DOI: 10.1088/1468-6996/13/6/064206.
(50) Chen, G. H.; Hoffman, A. S. Graft-Copolymers that Exhibit Temperature-Induced Phase-Transitions Over a Wide-Range of pH. *Nature* **1995**, *373*, 49−52.
(51) Duan, Q.; Miura, Y.; Narumi, A.; Shen, X.; Sato, S.-I.; Satoh, T.; Kakuchi, T. Synthesis and Thermoresponsive Property of End-Functionalized Poly(*N*-isopropylacrylamide) with Pyrenyl Group. *J. Polym. Sci., Part A: Polym. Chem.* **2006**, *44*, 1117−1124.
(52) Furyk, S.; Zhang, Y.; Ortiz-Acosta, D.; Cremer, P. S.; Bergbreiter, D. E. Effects of End Group Polarity and Molecular Weight on the Lower Critical Solution Temperature of Poly(*N*-isopropylacrylamide). *J. Polym. Sci., Part A: Polym. Chem.* **2006**, *44*, 1492−1501.
(53) Xia, Y.; Burke, N. A. D.; Stöver, H. D. H. End Group Effect on the Thermal Response of Narrow-Disperse Poly(*N*-isopropylacrylamide) Prepared by Atom Transfer Radical Polymerization. *Macromolecules* **2006**, *39*, 2275−2283.
(54) Xue, C.; Yonet-Tanyeri, N.; Brouette, N.; Sferrazza, M.; Braun, P. V.; Leckband, D. E. Protein Adsorption on Poly(*N*-isopropylacrylamide) Brushes: Dependence on Grafting Density and Chain Collapse. *Langmuir* **2011**, *27*, 8810−8818.
(55) Ko, H.; Zhang, Z.; Chueh, Y.-L.; Saiz, E.; Javey, A. Thermoresponsive Chemical Connectors Based on Hybrid Nanowire Forests. *Angew. Chem., Int. Ed.* **2010**, *49*, 616−619.
(56) Montagne, F.; Polesel-Maris, J.; Pugin, R.; Heinzelmann, H. Poly(*N*-isopropylacrylamide) Thin Films Densely Grafted onto Gold Surface: Preparation, Characterization, and Dynamic AFM Study of Temperature-Induced Chain Conformational Changes. *Langmuir* **2008**, *25*, 983−991.
(57) Makin, S. A.; Beveridge, T. J. *Pseudomonas aeruginosa* PAO1 Ceases to Express Serotype-Specific Lipopolysaccharide at 45 Degrees C. *J. Bacteriol.* **1996**, *178*, 3350−2.
(58) Gilboa-Garber, N.; Sudakevitz, D. The Hemagglutinating Activities of *Pseudomonas aeruginosa* Lectins PA-IL and PA-IIL Exhibit Opposite Temperature Profiles Due to Different Receptor Types. *FEMS Immunol. Med. Microbiol.* **1999**, *25*, 365−369.
(59) Makin, S. A.; Beveridge, T. J. The Influence of A-band and B-band Lipopolysaccharide on the Surface Characteristics and Adhesion of *Pseudomonas aeruginosa* to Surfaces. *Microbiology* **1996**, *142*, 299−307.
(60) Roosjen, A.; van der Mei, H. C.; Busscher, H. J.; Norde, W. Microbial Adhesion to Poly(ethylene oxide) Brushes: Influence of Polymer Chain Length and Temperature. *Langmuir* **2004**, *20*, 10949−10955.
(61) Zeraik, A. E.; Nitschke, M. Influence of Growth Media and Temperature on Bacterial Adhesion to Polystyrene Surfaces. *Braz. Arch. Biol. Technol.* **2012**, *55*, 569−576.
(62) Sun, L.; Zeng, X.; Yan, C.; Sun, X.; Gong, X.; Rao, Y.; Yan, N. Crystal Structure of A Bacterial Homologue of Glucose Transporters GLUT1-4. *Nature* **2012**, *490*, 361−366.
(63) Sage, A. E.; Proctor, W. D.; Phibbs, P. V. A Two-Component Response Regulator, GltR, Is Required for Glucose Transport Activity in *Pseudomonas aeruginosa* PAO1. *J. Bacteriol.* **1996**, *178*, 6064−6066.
(64) Lundquist, J. J.; Toone, E. J. The Cluster Glycoside Effect. *Chem. Rev.* **2002**, *102*, 555−578.
(65) Lee, Y. C.; Lee, R. T. Carbohydrate-Protein Interactions: Basis of Glycobiology. *Acc. Chem. Res.* **1995**, *28*, 321−327.
(66) Munoz, E. M.; Correa, J.; Fernandez-Megia, E.; Riguera, R. Probing the Relevance of Lectin Clustering for the Reliable Evaluation of Multivalent Carbohydrate Recognition. *J. Am. Chem. Soc.* **2009**, *131*, 17765−17767.
(67) Wang, Y.; Kotsuchibashi, Y.; Uto, K.; Ebara, M.; Aoyagi, T.; Liu, Y.; Narain, R. pH and Glucose Responsive Nanofibers for the Reversible Capture and Release of Lectins. *Biomater. Sci.* **2015**, *3*, 152−162.
(68) Wang, Y.; Kotsuchibashi, Y.; Liu, Y.; Narain, R. Temperature-Responsive Hyperbranched Amine-Based Polymers for Solid−Liquid Separation. *Langmuir* **2014**, *30*, 2360−2368.
(69) Hu, J.; Liu, S. Responsive Polymers for Detection and Sensing Applications: Current Status and Future Developments. *Macromolecules* **2010**, *43*, 8315−8330.

DOI: 10.1021/am508792k
ACS Appl. Mater. Interfaces 2015, 7, 1652−1661